Strong Spin-Orbit Interaction of Light in Plasmonic Nanostructures and Nanocircuits

Deng Pan,[1,2] Hong Wei,[2] Long Gao,[2] and Hongxing Xu[1,3,*]
[1]School of Physics and Technology, Wuhan University, Wuhan 430072, China
[2]Beijing National Laboratory for Condensed Matter Physics, Institute of Physics, Chinese Academy of Sciences, Beijing 100190, China
[3]Institute for Advanced Studies, Wuhan University, Wuhan 430072, China
(Received 12 August 2015; revised manuscript received 2 August 2016; published 12 October 2016)

The coupling between the spin and orbital degrees of freedom of photons is usually very weak, but recent studies have shown that this spin-orbit interaction (SOI) can be easily detected in metal structures. Here we show how the SOI of light is enhanced in plasmonic metal nanostructures, explore the underlying mechanism for this effect, and further demonstrate how it could potentially be harnessed for nanophotonic applications. Specifically, we show that the scattering of circularly polarized photons by a single metal nanosphere causes light to propagate along sharply twisted chiral trajectories near the nanosphere, thus revealing a strong SOI in the near field of surface plasmons. We find similar spin-dependent trajectories of light induced by a strong SOI also in the near field of surface plasmons generated on the tip of a metal nanowire. We utilize this strong SOI to for the first time experimentally realize spin sorting of photons in a compact plasmonic nanocircuit. The findings offer insights into how the SOI of light can be enhanced and explored for a new degree of freedom in plasmonic nanocircuits and future spin-controlled nanophotonic devices.

DOI: 10.1103/PhysRevLett.117.166803

When light interacts with a medium, the conservation of optical angular momentum (AM) can lead to a coupling between the photons' intrinsic spin degree of freedom and their orbital motion. An example manifestation of this spin-orbit interaction (SOI) of light is the transverse shift of circularly polarized beams when reflected by a dielectric interface [1,2]. Furthermore, previous studies have shown that the SOI of photons can lead to a series of spin-related optical phenomena [1–3] (for example, the photonic spin Hall effect (PSHE) [4–7]), and it has been conjectured that the spin AM of photons could be used as a new degree of freedom for processing optical information, whereby the SOI would be critical for controlling the sorting of signals [8]. However, the SOI of photons is usually very weak and the observation of SOI effects has typically relied on quantum weak measurements [6] or the accumulation of SOI in multiple reflections [7].

Recently, an alternative route to realizing and probing the SOI of photons has been explored in plasmonic nanostructures. For example, previous demonstrations of SOI effects of photons in plasmonic structures have included the spin-dependent distribution [9,10] and directional generation [11–13] of surface plasmon (SP) fields, the giant PSHE [14] and optical Rashba effect [15] on metasurfaces, and the metal nanoparticle as a chiral coupler for an ordinary dielectric waveguide [16]. So far, past studies have analyzed the SOI only in plasmonic structures based on the radiation from the dipole response of the structure observed in the far field [16,17]. However, the detailed knowledge on the process of the AM evolution in the strongly enhanced SOI in the near field of plasmonic nanostructures, which is important for exploring new SOI-based effects and devices, has so far been lacking. Moreover, although studies have, in principle, demonstrated the utilization of SOI for plasmonic devices [9–15], promising applications of the spin degree of freedom for optical information in plasmonics depend on the loading and sorting of circularly polarized photons in interconnected compact plasmonic nanocircuits [18,19]—this feature has to our knowledge not yet been realized and reported.

In this Letter, we tackle both of these issues. Specifically, we provide an intuitive picture of giant enhancement of a photonic SOI in the near field of plasmonic nanostructures, which offers in-depth insights into how the AM of photons evolves therein. Utilizing the obtained insights, we further design and demonstrate the sorting of circularly polarized photons in a compact plasmonic nanocircuit. To that end, we first study the simplest and most symmetric system, a metal nanosphere illuminated by circularly polarized photons, and show that photons in the SP near field follow dramatically twisted orbital trajectories, indicating the strong coupling between the photons' orbital and spin AM—we attribute this to the low circular polarization degree of the SP field. We find a similar strong SOI of photons, and the resulting transverse orbital momentum flows, in the SP field near the tip of a metal nanowire when excited by a circularly polarized light beam. Here, the localized SP field at the tip couples directionally to the propagating SP wave, leading to spin-controlled propagation on the metal nanowire. Based on this spin-controlled propagation, we for the first time experimentally realize the sorting of circularly polarized photons in a compact branched metal nanowire nanocircuit. These results not

only offer insights into the enhancement of the photonic SOI in plasmonic structures, but also offer a building block for the practical applications of signal processing using the spin degree of freedom of photons in plasmonic networks.

To describe the SOI of photons in plasmonic structures (see also Sec. I in Supplemental Material [20]), we first introduce the AM and the SOI of photons using a Dirac-like form of Maxwell's equation [21]:

$$c(\hat{\boldsymbol{\alpha}}\cdot\hat{\mathbf{p}})\Phi+\hat{\boldsymbol{\beta}}\mathbf{V}\Phi=i\partial/\partial t\Phi, \tag{1}$$

where c is the speed of light in vacuum; Φ is the field wave function formed by electric and magnetic fields $\Phi=\sqrt{(4\omega)^{-1}}[\sqrt{\varepsilon_0}\mathbf{E}\quad\sqrt{\mu_0}\mathbf{H}]^T$, where ω is the frequency of light; $\hat{\boldsymbol{\alpha}}_i$ $(i=1,\ 2,\ 3)$ and $\hat{\boldsymbol{\beta}}$ are the four Dirac matrices, among which the $\hat{\boldsymbol{\alpha}}_i$ are expressed using the spin-1 Pauli operators; $\hat{\mathbf{p}}$ is the ordinary momentum operator $-i\nabla$; $\mathbf{V}$ is the optical potential induced by the dielectric medium, which is $\omega[1-\varepsilon(\mathbf{r})]$ for nonmagnetic materials—in the case of a nanosphere, the potential can be viewed as a spherical potential well for photons.

Using this formalism, the local spin AM density is defined by $\langle\Phi|\boldsymbol{\alpha}|\Phi\rangle$, giving $\mathbf{s}=(4\omega)^{-1}\mathrm{Im}[\varepsilon_0\mathbf{E}^*\times\mathbf{E}+\mu_0\mathbf{H}^*\times\mathbf{H}]$. In turn, the orbital momentum density along the phase gradient is defined by $\langle\Phi|-i\nabla|\Phi\rangle$, explicitly as [22,23]:

$$\mathbf{p}^o=(4\omega)^{-1}\mathrm{Im}[\varepsilon_0\mathbf{E}^*(\nabla)\mathbf{E}+\mu_0\mathbf{H}^*(\nabla)\mathbf{H}]. \tag{2}$$

Here $\mathbf{p}^o$ is converted to the local wave vector when divided by the field intensity [24]. Finally, the orbital AM density is defined as $\mathbf{r}\times\mathbf{p}^o$ to describe the rotational motion, where $\mathbf{r}$ is the position vector. In this Letter, we adopt the orbital momentum density $\mathbf{p}^o$ and their streamlines to understand the photons and optical field in terms of trajectories or "currents." This is because the Poynting vector $\mathbf{S}=(1/2)\mathrm{Re}(\mathbf{E}^*\times\mathbf{H})=\mathbf{p}/c^2$ is not suitable, since the total momentum density $\mathbf{p}$ also includes the spin momentum density $\mathbf{p}^s=(\nabla\times\mathbf{s})/2$, which does not contribute to the energy transport. The orbital momentum density $\mathbf{p}^o$, on the other hand, corresponds to the photon trajectory, as measured by quantum weak measurements [25,26].

The coupling between the spin and orbital degrees of freedom of the photons is described by the term $\hat{\boldsymbol{\alpha}}\cdot\hat{\mathbf{p}}$ in Eq. (1). The SOI of photons is mediated by the optical potential, i.e., the permittivity for nonmagnetic materials, and its gradient—this is analogous to the mediation of the SOI of electrons by the gradient of the electric potential. This phenomenological picture is supported by the original paper on the PSHE [4], where the gradient of the permittivity introduces the SOI effect, and by a recent paper [27], in which a detailed derivation of the mathematical similarity between the SOI of photons and electrons reveals how the gradient of permittivity induces a photonic SOI. In this formalism, for light propagating in a dielectric medium, the SOI occurs because the gradient of permittivity influences the curl and thus the spin of electric field. In particular, strong SOI can be realized if there is a large dielectric material discrepancy, such as the one at the boundary of metal structures.

To illustrate how this type of strong SOI of photons can be induced in plasmonic nanostructures, we here first studied, theoretically, a simple gold nanosphere under the illumination of a circularly polarized electromagnetic plane wave (Fig. 1). To that end, we applied the finite element method (FEM) to obtain the field distributions (see Supplemental Material [20], Sec. II for details on the method) and calculated the orbital momentum density $\mathbf{p}^o$ using Eq. (2).

The streamlines resulting from our theoretical study are shown in Fig. 1(a) (simulation result for opposite circular polarization can be seen in Supplemental Material [20], Sec. III). Here, the tangents of the streamlines denote the direction of local orbital momentum density $\mathbf{p}^o$. For a circularly polarized incident wave, the orbital momentum density $\mathbf{p}^o$ is uniformly forward along the wave vector in the z direction. Interestingly, in the near field of the nanosphere, the orbital momentum density $\mathbf{p}^o$ gains azimuthal components and forms a vortex. This manifests as the streamlines of $\mathbf{p}^o$ twisting around the sphere, with the chirality of the spiral determined by the spin direction of the incident photons. We find that this type of chiral streamlines occurs for a wide range of wavelengths around the SP resonance peak (see Sec. IV in Supplemental Material [20]).

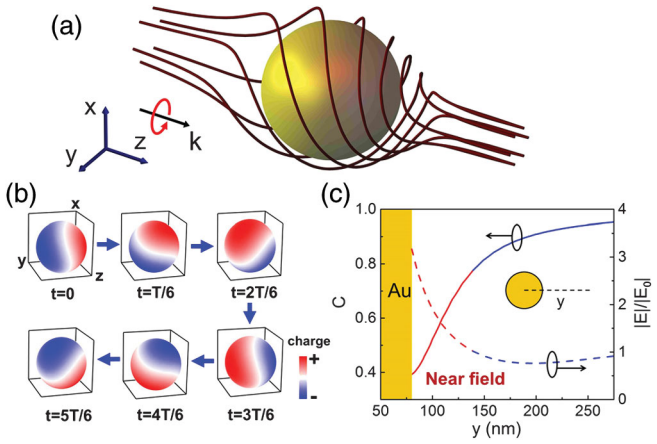

FIG. 1. A strong SOI in the scattering of circularly polarized photons on a single gold nanosphere. (a) Calculation results for streamlines of the orbital momentum density $\mathbf{p}^o$ during the scattering. (b) The surface charge-oscillation wave circulating around the nanosphere showing the orbital AM of the generated SPs. Six segments with equal intervals during one period T are shown. (c) The circular polarization degree C for the field near the nanosphere (solid curve) and the field enhancement (dashed curve). The wavelength is 785 nm, and the particle is a gold nanosphere with a radius $r=80$ nm embedded in a homogeneous dielectric medium ($n=1.5$).

The dramatically twisted chiral streamlines of $\mathbf{p}^o$ reveal that the photons' SOI is strongly enhanced in the SP near field—the intrinsic spin AM of the incident wave thus effectively couples to the orbital AM in the near field along the z direction, which results in the vortex flow. The direction of $\mathbf{p}^o$ is in accordance with the phase gradient of SPs, as revealed by the charge distributions on the nanosphere shown in Fig. 1(b). Here, the real-time evolution of the charge distributions indicates the generated SP wave acquires orbital AM and circulates around the nanosphere—this orbital AM is generated and mediated by the SOI process.

The strong SOI effect is also demonstrated by the polarization characteristics of the near field [Fig. 1(c)]. Here, the distribution of the field enhancement [dashed curve in Fig. 1(c)] shows that the SP field is well localized in the subwavelength scale outside the gold surface. Meanwhile, the circular polarization degree drops to a low value for the field near the gold surface [solid curve in Fig. 1(c)]. Here, we define the circular polarization degree as $C = |\varepsilon_0 \mathbf{E}^* \times \mathbf{E} + \mu_0 \mathbf{H}^* \times \mathbf{H}|/(\varepsilon_0|\mathbf{E}|^2 + \mu_0|\mathbf{H}|^2)$, fulfilling $C = 1$ for the circular polarization and $C = 0$ for the linear polarization. The low circular polarization degree of the field near the nanosphere, as compared to the incident light and the far field, implies that most of the spin AM of the photons is converted to the orbital AM by means of the SOI in this region.

To understand the origin of the strong photonic SOI in the plasmonic near field, we next present a description similar to that usually employed for paraxial beams. For paraxial beams, due to the orthogonality between the wave vector $\mathbf{k}$ and the field components, the flow of light in the curved trajectory will induce a geometric rotation of the polarization and a coupling between the photons' spin and orbital AM. In contrast, for the nonparaxial optical near field including evanescent components, no effective description has been proposed. However, in the near field of the metal nanosphere, due to the low circular polarization degree and corresponding smaller value of $\mathbf{p}^s$, the streamlines of the orbital momentum density $\mathbf{p}^o$ share a similar distribution as that of the Poynting vector $\mathbf{S}$ (see Sec. V in Supplemental Material [20]). Considering the requirement $\mathbf{S} \cdot \mathbf{E} = 0$, a similar constraint for $\mathbf{p}^o$ and $\mathbf{E}$ holds for the near field around the nanosphere. Therefore, similar to the paraxial beam, the bending of the orbital momentum density $\mathbf{p}^o$ is accompanied with a SOI, which induces an azimuthal shift of the streamlines and produces an orbital AM along the z direction. This azimuthal shift actually reveals the anomalous velocity induced by the geometric phase (see the more detailed discussion in Supplemental Material [20], Sec. VI). While the photonic SOI can also occur on a dielectric particle, it will be stronger for metal structures (see the comparison in Supplemental Material [20], Sec. VII). The strong enhancement of the photonic SOI around the metal nanoparticle occurs because of the large geometric phase associated with the sharply bent photon trajectory during the strong SP scattering on the opaque metal particle.

Our analysis of the enhancement of photonic SOI in the presence of a metal nanosphere is general and applicable to other metal structures. To illustrate this, we performed a similar theoretical analysis of a metal nanowire. We hereby illuminated one end of a gold nanowire with a Gaussian beam of circularly polarized light [Fig. 2(a)] and calculated the surface charge distribution and the streamlines of the $\mathbf{p}^o$ around the tip [Fig. 2(b)] using the FEM. We observed twisted orbital momentum density flow and transverse propagation of surface charge wave similar to the one seen in the metal nanosphere [Figs. 1(a) and 1(b)]. These largely twisted streamlines also result from the transverse momentum flow induced by the strong SOI process.

The transverse components of the orbital momentum density in the x-y plane resulting from the SOI lead to directional coupling to the propagating SPs on the nanowire [Fig. 2(c)] (simulation results for opposite circular polarization can be seen in Supplemental Material [20], Sec. VIII). When illuminated by the circularly polarized light beam, the SPs on the nanowire show a periodic zigzag pattern, with the nodes marked by the white dashed lines. Because of the transverse flow shown in Fig. 2(b), the field near the tip is concentrated on one side of the nanowire and forms the first node of the propagating SPs.

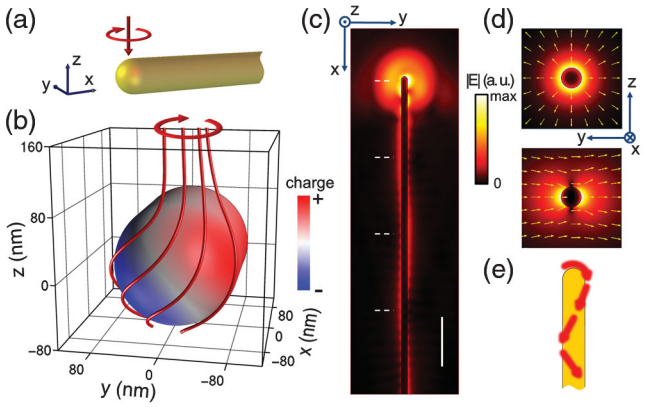

FIG. 2. The SOI and resulting spin-controlled propagation of SPs on a gold nanowire. (a) Schematic illustration for the excitation of SPs on a nanowire using circularly polarized photons. (b) The distributions of surface charges and the streamlines of $\mathbf{p}^o$ for the near field on the tip of a gold nanowire with a radius of 80 nm in a homogeneous dielectric medium ($n = 1.5$). The wavelength is 785 nm. (c) Sectional view of the electric field distribution on the x-y plane across the center of the nanowire. The scale bar is 1 μm. The white dashed lines mark the nodes in the periodic zigzag pattern. (d) Field distribution of two lowest order eigenmodes of the nanowire, with the arrows denoting the directions of the electric field. (c) and (d) share the same color bar with normalized color range. (e) Sketch for understanding the field distribution in (c) from the perspective of the ray trajectory.

The asymmetric field distribution on the nanowire can be decomposed into two fundamental waveguide modes of different symmetry [Fig. 2(d)] [28–33]. The period is decided by $\Lambda = \lambda_0/\mathrm{Re}(\Delta n)$, where λ_0 is the wavelength in vacuum and Δn is the difference of the effective refractive index of two modes. For the gold nanowire studied here, the effective refractive indexes of the two modes are 1.797 and 1.535, respectively, determining the period in Fig. 2(c) as 3 μm. In the perspective of photon trajectory shown by Fig. 2(e), the zigzag route of SPs can be viewed as an analogy of the multiple internal reflection at the boundary of an ordinary dielectric fiber following geometrical optics. Here the field distribution is determined by the SOI-resulted transverse power flow on the tip and will be reversed as the mirror image under an excitation beam with opposite circular polarization (experimentally demonstrated in Supplemental Material [20], Sec. IX). Therefore, the incident photons with different spin AM are separated into different spatial trajectories on the nanowire due to the SOI of light on the tip of the nanowire, similar to the PSHE [8].

We next demonstrate experimentally how the enhanced photon SOI and directional coupling of SPs discussed above can be used to sort light with different circular polarization into separate physical paths (Figs. 3 and 4). To that end, we fabricated a gold Y-branch structure on a quartz substrate using electron beam lithography [Fig. 3(a)]. For the optical measurements, we covered the sample with index-matching oil to form a uniform dielectric environment and used the vertical branch as the main branch for inputting SP signals.

We expected that opposite circularly polarized laser beams focused at the terminal of the main branch would generate propagating SPs with periodic patterns [Fig. 2(c)] of different distributions, which would then allow the sorting of spin-encoded input signals by tailoring the length of the input branch accordingly. Using the effective refractive index of the two eigenmodes of the fabricated nanowire calculated by the FEM, we estimated that the period of the periodic SP pattern for our experimental device would be 7.4 μm, and we designed the length of the main branch as half the period to ensure an asymmetric distribution of the field at the junction and, thus, to enable the sorting of the SPs on the main branch to one of the two output branches. Our modeling [Fig. 3(b)] (Supplemental Material [20], Sec. X shows the geometry for the simulation) predicted that photons of opposite circular polarization illuminating the tip of the input branch nanowire would be coupled directionally to propagating SPs and further separated into different branches, leading to the spin sorting of SP signals in the plasmonic nanocircuit (Supplemental Material [20], Sec. XI shows it is possible to retrieve the spin polarizations for the emitted photons at the output terminals of our branched nanowire).

We experimentally demonstrate the predicted spin-sorting functionality in our fabricated branched-nanowire structure (Fig. 4). Here, a linearly polarized laser beam was focused onto the bottom terminal of the Y-branch structure with the polarization parallel with the nanowire. By rotating a quarter-wave plate inserted into the path of the laser light, we changed the polarization to circular polarization states σ^- (45°) and σ^+ (135°). The probed emission intensities on both output

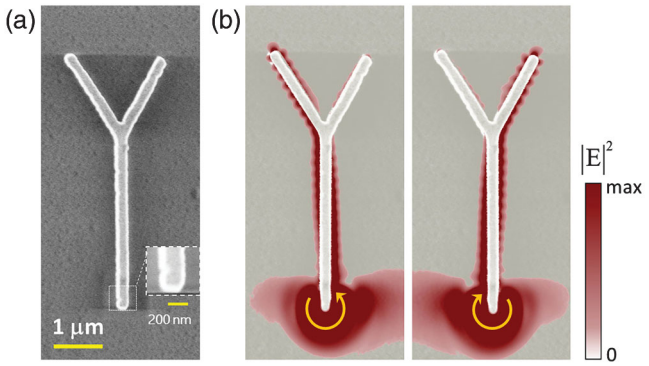

FIG. 3. Spin-dependent directional propagation of SPs in a gold branched nanowire. (a) Scanning electron microscopy (SEM) image of the fabricated gold branched-nanowire structure. The gold nanowire is about 260 nm wide and 150 nm thick. The length of the main wire is about 3.7 μm. (b) The SEM image in (a) overlaid with the simulated near-field distributions for excitations of 785 nm wavelength with different circular polarizations denoted by the circular arrows. A uniform dielectric environment ($n = 1.5$) is used for the simulation, and the field distributions are extracted from the central horizontal section of the structure.

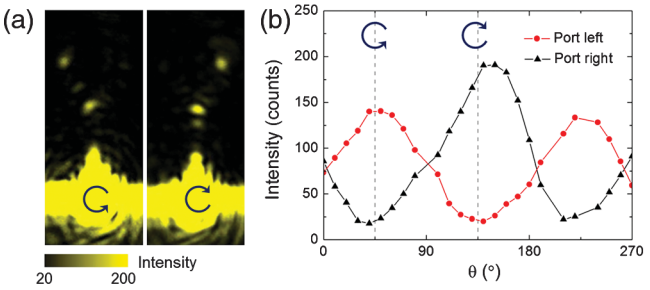

FIG. 4. An experimental demonstration of spin sorting in a plasmonic nanocircuit. (a) Scattering images for excitation by focused laser beams of 785 nm wavelength with opposite circular polarizations denoted by the circular arrows. The color scale is saturated to clearly show the outputs (the nonsaturated figure is shown in Supplemental Material [20], Sec. XII). (b) Measured intensities from the two output ports of the branched-nanowire structure for varying angle θ between the optical axis of the quarter-wave plate and the linear polarization of the laser beam. The $\theta = 0^o$, 90°, 180°, and 270° in (b) correspond to linear polarization parallel to the main nanowire of the Y-branch structure, while $\theta = 45^o$ and 135° correspond to circularly polarized light with opposite spins as denoted by the circular arrows.

branches, as a function of the rotation angle of the quarter-wave plate, reveal results that are consistent with our simulations, i.e., that the SPs generated by photons with opposite circular polarizations are effectively directed to different branches in the experiment (Supplemental Material [20], Sec. XIII shows that the linear polarizations can not be sorted in our sample), with the intensity ratio between two output ports higher than 6:1. The results demonstrate a novel approach to loading and sorting optical information, encoded in the spin degree of freedom of photons, in plasmonic nanocircuits.

In summary, in this Letter, we provide insights into how the SOI of photons can be strongly enhanced in plasmonic nanostructures and how this effect could be used to achieve new functionalities in nanophotonic circuits. Specifically, we have studied the evolution of the AM of light during the interaction between circularly polarized photons and individual metal nanostructures, and found that light propagates along chiral trajectories in the near field of SPs because of a strong SOI. This effect can be readily used to encode, transport, and manipulate the spin degree of freedom of optical information in nanophotonic and plasmonic circuits, as demonstrated by our proof-of-principle experiments on spin sorting in a plasmonic nanocircuit.

This work was supported by Ministry of Science and Technology of China (Grant No. 2015CB932400), National Natural Science Foundation of China (Grants No. 11134013, No. 11227407, No. 11374012, and No. 11422436), and "New Star of Science and Technology Program" of Beijing Municipal Science and Technology Commission. We thank Professor Peter Nordlander for the helpful discussion.

*hxxu@whu.edu.cn

[1] F. I. K. Fedorov, Dokl. Akad. Nauk SSSR **105**, 465 (1955).
[2] C. Imbert, Phys. Rev. D **5**, 787 (1972).
[3] A. V. Dooghin, N. D. Kundikova, V. S. Liberman, and B. Y. Zeldovich, Phys. Rev. A **45**, 8204 (1992).
[4] M. Onoda, S. Murakami, and N. Nagaosa, Phys. Rev. Lett. **93**, 083901 (2004).
[5] K. Y. Bliokh and Y. P. Bliokh, Phys. Rev. Lett. **96**, 073903 (2006).
[6] O. Hosten and P. Kwiat, Science **319**, 787 (2008).
[7] K. Y. Bliokh, A. Niv, V. Kleiner, and E. Hasman, Nat. Photonics **2**, 748 (2008).
[8] K. Y. Bliokh, F. J. Rodríguez-Fortuño, F. Nori, and A. V. Zayats, Nat. Photonics **9**, 796 (2015).
[9] Y. Gorodetski, A. Niv, V. Kleiner, and E. Hasman, Phys. Rev. Lett. **101**, 043903 (2008).
[10] K. Y. Bliokh, Y. Gorodetski, V. Kleiner, and E. Hasman, Phys. Rev. Lett. **101**, 030404 (2008).
[11] S. Y. Lee, I. M. Lee, J. Park, S. Oh, W. Lee, K. Y. Kim, and B. Lee, Phys. Rev. Lett. **108**, 213907 (2012).
[12] F. J. Rodriguez-Fortuno, G. Marino, P. Ginzburg, D. O'Connor, A. Martinez, G. A. Wurtz, and A. V. Zayats, Science **340**, 328 (2013).
[13] J. Lin, J. P. B. Mueller, Q. Wang, G. Yuan, N. Antoniou, X.-C. Yuan, and F. Capasso, Science **340**, 331 (2013).
[14] X. B. Yin, Z. L. Ye, J. Rho, Y. Wang, and X. Zhang, Science **339**, 1405 (2013).
[15] N. Shitrit, I. Yulevich, E. Maguid, D. Ozeri, D. Veksler, V. Kleiner, and E. Hasman, Science **340**, 724 (2013).
[16] J. Petersen, J. Volz, and A. Rauschenbeutel, Science **346**, 67 (2014).
[17] D. O'Connor, P. Ginzburg, F. J. Rodríguez-Fortuno, G. A. Wurtz, and A. V. Zayats, Nat. Commun. **5**, 5327 (2014).
[18] S. I. Bozhevolnyi, V. S. Volkov, E. Devaux, J. Y. Laluet, and T. W. Ebbesen, Nature (London) **440**, 508 (2006).
[19] D. K. Gramotnev and S. I. Bozhevolnyi, Nat. Photonics **4**, 83 (2010).
[20] See Supplemental Material at http://link.aps.org/supplemental/10.1103/PhysRevLett.117.166803 for technical details, more simulation results, experimental results for spin-controlled SP propagation, and additional discussions.
[21] E. Mignani, E. Recami, and M. Baldo, Lett. Nuovo Cimento **11**, 568 (1974).
[22] M. V. Berry, J. Opt. A **11**, 094001 (2009).
[23] K. Y. Bliokh, A. Y. Bekshaev, and F. Nori, Nat. Commun. **5**, 3300 (2014).
[24] J. F. Nye, *Natural Focusing and Fine Structure of Light: Caustics and Wave Dislocations* (Institute of Physics, Bristol, 1999).
[25] S. Kocsis, B. Braverman, S. Ravets, M. J. Stevens, R. P. Mirin, L. K. Shalm, and A. M. Steinberg, Science **332**, 1170 (2011).
[26] K. Y. Bliokh, A. Y. Bekshaev, A. G. Kofman, and F. Nori, New J. Phys. **15**, 073022 (2013).
[27] C. C. Leary and K. H. Smith, Phys. Rev. A **89**, 023831 (2014).
[28] S. P. Zhang, H. Wei, K. Bao, U. Hakanson, N. J. Halas, P. Nordlander, and H. X. Xu, Phys. Rev. Lett. **107**, 096801 (2011).
[29] H. Wei, Z. P. Li, X. R. Tian, Z. X. Wang, F. Z. Cong, N. Liu, S. P. Zhang, P. Nordlander, N. J. Halas, and H. X. Xu, Nano Lett. **11**, 471 (2011).
[30] Y. R. Fang, Z. P. Li, Y. Z. Huang, S. P. Zhang, P. Nordlander, N. J. Halas, and H. X. Xu, Nano Lett. **10**, 1950 (2010).
[31] H. Wei, Z. X. Wang, X. R. Tian, M. Käll, and H. X. Xu, Nat. Commun. **2**, 387 (2011).
[32] H. Wei, S. P. Zhang, X. R. Tian, and H. X. Xu, Proc. Natl. Acad. Sci. U.S.A. **110**, 4494 (2013).
[33] D. Pan, H. Wei, Z. L. Jia, and H. X. Xu, Sci. Rep. **4**, 4993 (2014).